NOTICE: This is the author's version of a work that was accepted for publication in Tectonophysics. Changes resulting from the publishing process, such as peer review, editing, corrections, structural formatting, and other quality control mechanisms may not be reflected in this document. Changes may have been made to this work since it was submitted for publication. A definitive version was subsequently published in Tectonophysics [482, 1-4, 2010] DOI 10.1016/j.tecto.2009.07.021

Present-Day Stress Orientation in the Molasse Basin

John Reinecker[a*], Mark Tingay[b], Birgit Müller[c,d] and Oliver Heidbach[d,e]

[a]*Institute for Geosciences, University of Tübingen, Sigwartstr. 10, 72076 Tübingen, Germany*
[b]*Department of Applied Geology, Curtin University of Technology, Perth, 6845 WA.*
[c]*Heidelberg Academy of Sciences and Humanities, Karlstr.4, 9117 Heidelberg, Germany*
[d]*Geophysical Institute, University of Karlsruhe, Hertzstr.16, 76187 Karlsruhe, Germany*
[e]*now at German Research Centre for Geosciences, Telegrafenberg, 14473 Potsdam, Germany*

Abstract

The present-day state of stress in Western Europe is considered to be controlled by forces acting at the plate boundaries. It is assumed that the Alpine orogen only influence the regional pattern of present-day stress in Western Europe within the Alps themselves. We examine the present-day maximum horizontal stress orientation in the Molasse Basin in the Alpine foreland in order to investigate the possible influence of the Alps on the far-field stress pattern of Western Europe. Four-arm caliper and image logs were analysed in 137 wells, in which a total of 1348 borehole breakouts and 59 drilling-induced fractures were observed in 98 wells in the German Molasse Basin. The borehole breakouts and drilling-induced fractures reveal that stress orientations are highly consistent within the Molasse Basin and that the present-day maximum horizontal stress orientation rotates from N-S in southeast Germany (002ºN ± 19º) to approximately NNW-SSE in southwest Germany and the Swiss Molasse Basin (150ºN ± 24º). The present-day maximum horizontal stress orientation in the Molasse Basin is broadly perpendicular to the strike of the Alpine front, indicating that the stress pattern is probably controlled by gravitational potential energy of Alpine topography rather than by plate boundary forces. The present-day maximum horizontal stress orientations determined herein have important implications for the production of hydrocarbons and geothermal energy in the German Molasse Basin, in

particular that hydraulically-induced fractures are likely to propagate N-S and that wells deviated to the north or south may have reduced wellbore instability problems.

Keywords: stress field; borehole breakouts; drilling induced fractures; tectonics; Molasse Basin

1. Introduction

The present-day stress field of Western Europe is considered to be primarily controlled by resistance forces generated by Eurasia-Africa plate collision and ridge-push forces exerted by the mid-Atlantic spreading centre (Müller et al., 1992; Zoback, 1992; Grünthal and Stromeyer, 1986). The first-order control of the Europe-Africa boundary and the mid-Atlantic Ridge on the stress field in Western Europe is supported by the predominantly NW-SE present-day maximum horizontal stress (S_H) orientation (mean S_H orientation of 144°N; Müller et al., 1992; Heidbach et al., 2007), the observation that S_H is sub-parallel to relative plate motion (Müller et al., 1992; Richardson, 1992) and by means of plate-scale finite element modelling of the stress field (Grünthal and Stromeyer, 1992; Gölke and Coblentz, 1996). However, these models downplay the influence of intraplate sources of stress, particularly the Alpine orogen, on the stress field in Western Europe.

The plate boundary driven models of stress in Europe have been used to suggest that forces generated by the Alpine orogen have only a negligible impact on the Western European stress field, resulting only in extensional stresses within the Alps themselves (Zoback, 1992; Gölke and Coblentz, 1996). However, the Alpine orogen has had a dominant and widespread far-field influence on the Cenozoic tectonics in Western Europe (Cloetingh, 1986; Ziegler, 1987). Illies and Greiner (1978) postulate that the S_H orientations are approximately perpendicular to the isobases of Holocene uplift in the Rhine Graben. Stresses generated by the Alpine orogen are hypothesised to have been transmitted over 1500 kilometres from the Alps, resulting in uplift and inversion in numerous areas such as the UK and southern North Sea (Cloetingh, 1986; Ziegler 1990; Hillis et al., 2008). Furthermore, recent compilations of S_H orientations reveal that the stress pattern in Western Europe is less homogeneous than previously assumed. The wave-lengths of the stress pattern range from tens to hundreds of kilometres (Müller et al., 1997; Tingay et al., 2006; Heidbach et al., 2007; Heidbach et al., this issue). These second- and third-order stress pattern indicate that localised intraplate sources of stress, such as gravitational potential energy of the elevated Alpine orogen as well as lateral density and strength contrasts can locally overrule the far-field stress contribution in Western Europe and determine the S_H orientations (Tingay et al., 2006; Heidbach et al., 2007).

The new data from the Molasse Basin, immediately adjacent to the Alps, provides an opportunity to better understand the relative influence of the Alpine orogen on the European stress pattern. The plate boundary driven models suggest that the Alpine orogen generates only minor gravitational forces localised within the Alps and that a NW-SE to NNW-SSE S_H pattern should be observed throughout the Alpine foreland (and most of Germany and France; Gölke and Coblentz, 1996). However, the S_H orientation would be expected to be roughly perpendicular to the Alpine front (rotating from N-S in southeast Germany to approximately NNW-SSE in southwest Germany) if gravitational and collisional resistance forces generated by the Alps are significantly influencing the stress pattern in the Alpine foreland.

In this study we conduct the first regional investigation of the present-day S_H orientation in the German Molasse Basin. We use borehole breakouts interpreted from four-arm caliper and image log data from hydrocarbon and geothermal wells. We discuss localised stress variations, the stress regime, and the sources of the stress field.

2. Geology and tectonic evolution

The Molasse Basin, located immediately north of the Alps, is considered a classical peripheral foreland basin. It extends over a lateral distance of approximately 1000 km from Lake Geneva in the west to Lower Austria in the east and has a present-day maximum width of 130 km in Bavaria, SE Germany (Fig. 1). The basin has a typically asymmetric cross-section with its deepest part along the Alpine thrust front in SE Bavaria. The Molasse Basin is filled with up to 5000 m of predominantly Late Eocene to Late Miocene sediments of different facies, comprising fluvial fans to deep-marine sandstones, marls and clays (Fig. 1; see Bachmann et al., 1982; Bachmann et al., 1987, and Kuhlemann and Kempf, 2002 for details on basin evolution). The Tertiary strata are underlain by 500-1000 m of Mesozoic shelf sediments, local Permo-Carboniferous troughs containing unknown thicknesses of clastics, and the Variscan basement.

Basin formation and sedimentation is primarily due to the northward thrusting and isostatic uplift of Alpine nappes and associated down bending of the European plate. At smaller scales, basin formation has been influenced by the inherited structures of the pre-Tertiary basement (Bachmann et al., 1987). Subsidence of the Molasse Basin was initiated and controlled by Alpine nappe tectonics in the south and resulted in formation of E-W striking normal faults that are currently inactive. Over the course of basin evolution, Alpine nappes were thrust northward by up to 50 km onto the Molasse sediments (Bachmann et al., 1987). During thrusting, Molasse sediments in the south became subsequently incorporated into Alpine nappe tectonics (‘Subalpine Molasse’), in contrast to the more or less undisturbed

'Autochthonous Molasse' in the north and below the Subalpine Molasse. Betz and Wendt (1983) and Brink et al. (1992) describe broad anticlines in the Swiss Molasse Basin, which are very rare in the German part, probably because of the absence of preferred décollement horizons like the Muschelkalk evaporites in Switzerland. Compressive stresses resulting in these folds are believed to result form the northward propagation of Alpine nappes and the topography of the orogen (Illies and Greiner, 1978).

3. Stress orientation from borehole breakout and drilling-induced fracture analysis

The S_H orientation in the Molasse Basin was determined herein from borehole breakouts (BO) and drilling-induced fractures (DIF). Breakouts are stress-induced enlargements of the wellbore cross-section (Bell and Gough, 1979). When a wellbore is drilled, the material removed from the subsurface is no longer supporting the surrounding rock. As a result, the stresses become concentrated in the surrounding rock (i.e. the wellbore wall). Borehole breakout occurs when stresses around the borehole exceed the compressive strength of the borehole wall (Zoback et al., 1985; Bell, 1990). The enlargement of the wellbore is caused by the development of intersecting conjugate shear planes that cause pieces of the borehole wall to spall off (Zoback et al., 1985). The stress concentration around a vertical borehole is greatest in the direction of the minimum horizontal stress (S_h). Hence, the long axes of borehole breakouts are oriented approximately perpendicular to the S_H orientation. DIF's are created when the stresses concentrated around a borehole exceed the tensile strength of the wellbore wall (Aadnoy, 1990). DIF's typically develop as narrow sharply defined features that are sub-parallel or slightly inclined to the borehole axis in vertical wells. The stress concentration around a vertical borehole is at a minimum in the S_H direction. Hence, DIF's develop approximately parallel to the S_H orientation (Aadnoy and Bell, 1998).

Borehole breakouts are interpreted in this study from the analysis of four-arm caliper log data from 132 wells (Table 1). The interpretation of borehole breakouts from caliper log data is conducted using the standard breakout interpretation methodology, with all breakouts being manually interpreted (Bell and Gough, 1979; Plumb and Hickman, 1985; Zoback et al., 1985; Reinecker et al., 2003). Image logs are available from five wells, from which we are able to visually identify DIF's as well as borehole breakout (Tingay et al., 2008). All but 15 wells in the study are sub-vertical and no stress-induced features were included from wells with deviations greater than 5° from vertical if the hole elongation azimuth was within 15° of the hole deviation direction. The average S_H orientation and standard deviation of the stress-induced features observed in each well are calculated using circular statistical analysis following Mardia (1972). The average S_H orientations for each well are quality-ranked according to the updated World Stress Map criteria and available in the World Stress Map 2008 database release (Heidbach et al., 2008; Heidbach et al., this issue).

4. Stress field in the German Molasse Basin

Approximately 167 kilometres of four-arm caliper and 2.5 kilometres of image log data are analysed from the German Molasse Basin, revealing a total of 1348 breakouts and 59 DIF's in 98 wells (Table 1). S_H orientations from 67 wells are ranked A-C quality and used in the analysis herein (Table 1; Fig. 2; Fig. 3). The borehole breakouts and DIF's interpreted herein indicate a highly uniform north-south S_H orientation (average 002ºN with standard deviation of 19.2º; Fig. 2C) within the Molasse Basin and below in the pre-Tertiary basement. Some wells show perturbed S_H orientations from the dominant N-S orientation but without any regional trend within the Molasse Basin. Localized stress perturbations can be caused by proximity to nearby faults or other structures and in most cases the wells with possible stress rotations are of low quality (see discussion below). No significant rotation of S_H orientation with depth is found from this analysis (Fig. 3A,C). The high ratio between breakouts and well log lengths (with values up to 65 %; Fig. 3B,D) show that horizontal differential stresses ($S_{HD} = S_H$-S_h) are sufficiently high to create breakouts within large volumes of the Molasse Basin.

The N-S S_H orientation observed in most of the German Molasse Basin is consistent with the S_H orientation estimated from pressure solution of pebbles in Molasse Basin sequences (Schrader, 1988). S_H orientations estimated from earthquake focal mechanisms below the western part of the German Molasse Basin show the same N-S compression, suggesting that the regional S_H orientations do not vary significantly at crustal scale (Fig.4; Müller et al., 1997; Kastrup et al., 2004).

5. Discussion

Localised variations of S_H orientation

Most of the analysed wells are drilled by oil and gas exploration companies. Within the German Molasse Basin structural traps are commonly characterised by partly sealing E-W to NE-SW striking synthetic and antithetic normal faults (Brink et al. 1992). Therefore the proximity of these structures is quite likely to locally perturb the stress field in some locations.

Localised variations of up to 90° from the regional N-S S_H trend are observed in Illmensee 5 and 8, Mönchsrot 26, Tacherting 1b, Aitingen 4a, Höhenrain A5, Schmidhausen A3, Inzenham-West 14, Breitbrunn C10, Schnaitsee 7, Vorderriss 1, and Hindelang 3L (all of

A-C quality; Fig. 2A,B; Table 1). All, but the latter two are drilled within the foreland Molasse Basin.

The observed breakout zones in wells Hindelang 3L and Vorderriss 1 are located within the Alpine thrust belt (Fig. 2A and 3A; Table 1). In the lowest part Hindelang 3L has reached the allochthonous (folded) Molasse. The S_H orientation is consistently NW-SE in these two wells, but with a high standard deviation of 22°. The origin of this NW-SE S_H orientation is unknown. However, the high standard deviation of the S_H orientations may reflect local perturbations due to the complex structure of the penetrated Alpine nappe stack. From modelling studies we can exclude an influence of the sharp topographic relief in intramontane regions on S_H orientation at depth greater than 500 m (Engelder, 1993). Lithostatic overpressures, as observed in Hindelang 3L, may indicate either rapid sedimentary or tectonic loading, or a high degree of shearing. The latter is believed to be the case for Hindelang 3L and may be accompanied by additional lateral stress (Müller and Nieberding, 1995, 1996). Here the breakouts occur in the zone of overpressure, but due to lack of data we can not exclude breakouts to be present in zones of normal pressure. In contrast Vorderriss 1 does not show overpressures. However, the quality of sealing, which depends on the structural geology and lithology, seems critical to encounter overpressures (Müller and Nieberding, 1995, 1996). So up to now we can not explain the NW-SE S_H orientation observed in these two wells.

The field Illmensee is located in the westernmost part of the German Molasse Basin. The local stress field there is the least constrained in the study area. Nearby wells show very different S_H orientations. Illmensee 6 and 7 fit in the regional N-S trend of the S_H orientation. Illmensee 8 and 5 instead indicate E-W and NE-SW S_H orientations, respectively (Figure 2A,B; Table 1). However, further to the east a clear N-S S_H orientation is observed in the wells Ravensburg 1, Grünlingen 1, and Frohnhofen 16 (Fig. 2A).

The wells Mönchsrot 26 and Tacherting 1b contain breakouts indicating approximately E-W S_H orientations at relatively shallow depths (<1900 m), although N-S S_H orientations are observed in deeper sequences of these and nearby wells (Fig. 2A,B and 3A; Table 1).

The analysed log intervals from the wells Schmidhausen A3, Inzenham-West 14, Höhenrain A5, and the uppermost section of Breitbrunn C10 are all short, very shallow (<1000 m), and indicate NE-SW S_H orientations (Figure 2A,B; Table 1). Aitingen 4a is the only well showing NW-SE S_H orientation within the German Molasse Basin (Figure 2A; Table 1). In all cases we are not able to address stratigraphic correlation of the abnormal stress orientations, but nearby wells clearly indicate N-S S_H orientation with a high quality at comparable depths suggesting that active faults at depth probably locally perturb the S_H orientation.

Schnaitsee 7 is the only well where we have evidence for abrupt rotation of the S_H orientation from N-S within the Molasse sequences to NW-SE in the underlying Mesozoic strata. The NW-SE S_H orientation is of only D-quality and should therefore not be over interpreted.

We can not exclude the possibility that these abnormal S_H orientations may be artefacts resulting from large DIF's being incorrectly interpreted as breakouts on four-arm caliper log data. An accurate distinction between breakouts and large DIF's can only be made from high resolution image logs, which are rarely run in the Molasse Basin during the main period of exploration activity between 1970 and 1990.

Estimates of the relative state of stress in the Molasse Basin

No data was available for this study to directly examine stress magnitudes. However, it is possible to speculate on the state of stress in the German Molasse Basin based on the stress pattern and further details of the wellbore failure observations. Over 1300 breakouts are interpreted in this study and breakouts were often observed to have large angular widths (>60º), high eccentricities (>50% more than bit size) and occur at shallow depths (at <600 m depth in 27 wells, with some breakout observed at less than 100 m depth).

Breakouts and DIF's require high horizontal stresses and, typically, horizontal stress differences to develop (Engelder, 1993; Haimson and Herrick, 1989). Breakout width and eccentricity have been used to give an indication on the magnitude of horizontal differential stress (Zoback et al., 1985; Haimson and Herrick, 1989). Laboratory studies suggest that the width of breakouts in vertical wells is proportional to the ratio of the two horizontal principal stresses S_H/S_h and can help constrain the in-situ stress tensor (Zoback et al., 1985; Barton et al., 1988; Zajak and Stock, 1997). Hence, breakouts that exhibit high angular widths can be used as a rough proxy for the value of S_{HD} (Zoback et al., 1985; Haimson and Herrick, 1989; Engelder, 1993). The high angular widths and eccentricities of breakouts observed in this study suggest that S_{HD} values are high in the Molasse Basin.

The four-arm caliper log datasets examined herein contain, rather unusually, a significant number of logging runs at very shallow depth, with 43 wells containing caliper log at depths shallower than 500 m. Furthermore, the shallow caliper log data examined herein revealed that breakouts in the German Molasse Basin occur at very shallow depths, with the shallowest breakout observed at just 67 m below the surface. Breakouts are rarely observed at such shallow depths, particularly in petroleum wells in which the pressure of the drilling mud improves the stability of the wellbore. In general, the S_{HD} in shallow sedimentary sequences are typically too low to induce failure. Furthermore, shallow sediments are unconsolidated and weak and thus unable to transmit high magnitudes of shear stress. Hence, the unusual observation of breakouts at shallow depths suggests that the horizontal stress magnitudes (or, at least S_H magnitude) are quite high in the Molasse Basin.

The occurrence of small-scale stress perturbations, such as those discussed in the previous section, is frequently considered to indicate that horizontal stress magnitudes are relatively similar and/or that local intra-basinal sources of stress dominate over far-field sources (Sonder, 1990; Bell, 1996; Tingay et al., 2006). However, the inference of similar S_H and S_h magnitudes due to the presence of small-scale stress perturbations is inconsistent with the observations of wellbore failure at low depth discussed above.

The majority of stress regimes inferred from earthquake focal mechanisms, recent structural styles in the region, and observations of thrust deformation in the lignite mine of Peissenberg (Heissbauer, 1975; Illies and Greiner, 1978) indicate that a strike-slip or thrust faulting stress regime is most likely present in the Molasse Basin (Fig. 4). Therefore, we speculate that the characteristics of wellbore failure, combined with the observed recent structural and fault styles, indicate that a strike-slip ($S_H>S_v>S_h$) or thrust ($S_H>S_h>S_v$) faulting stress regime presently exists in the German Molasse Basin.

Sources of the North Alpine foreland stress field

Plate boundary forces resulting from northward motion and counter clockwise rotation of Adria relative to stable Europe, together with push from the north Atlantic mid ocean ridge, are commonly suggested to control the stress field in central and western Europe (e.g. Müller et al., 1992). On the other hand, stresses resulting from buoyancy forces associated with elevated topography and related thickened crust of the Alps may also significantly contribute to the stress pattern in the north Alpine foreland.

The general pattern of S_H orientations within the Molasse Basin is perpendicular to the strike of the Alpine front in the near vicinity north of the Alps between Lake Geneva and Salzburg (Fig. 2A,B and 4; Kastrup et al., 2004). WNW-ESE S_H orientations found in the eastern Swiss Molasse Basin and the eastern Jura Mountains (Becker, 2000) are controlled by the influence of the Black Forest Massif. Further to the east (between Salzburg and Vienna), the stress pattern seems to be regionally perturbed by the Bohemian Massif acting as a rigid indenter (Reinecker and Lenhardt, 1999).

S_H orientations change with depth in the western Swiss Molasse Basin due to Mesozoic evaporite layers below the Molasse Basin, which are acting as décollement horizons (e.g. Brereton and Müller, 1991). However, no such evaporitic layers are known to occur in the German Molasse Basin and no systematic stress rotations with depth are observed in the German Alpine foreland. The well Bromberg 1 (Fig. 3A) is a nice example for a continuous stress profile from the Tertiary Molasse Basin into the underlying Mesozoic strata indicating N-S S_H orientation down to 4.7 km depth. The observed overpressures in this well have no effect on the S_H orientation (Müller and Nieberding, 1996). Also the wells Grambach 1 and Bad Waldsee 2 provide further evidence that S_H orientations are generally N-S in the German Molasse Basin and below to depths of 6 km (Fig. 3A,C). S_H orientations from earthquake focal mechanisms in the western German Molasse Basin support this hypothesis (Fig. 4).

The observation that S_H is oriented perpendicular to the Alpine front, and not restricted to the Molasse sediment sequence, indicates that the present-day stress pattern in the foreland is probably controlled by the gravitational potential energy generated by Alpine topography. Furthermore, the N-S S_H orientation is observed over 100 km from the Alpine front, suggesting that topographic stresses can be transmitted larger distances away from mountain ranges (Fig. 2, Fig.4).

In-situ stresses at any given point are the combined result of far-field and local sources of stress, and thus, stress orientations should typically not be considered to result from only one source of stress (Sonder, 1990; Tingay et al., 2006). Hence, although gravitational forces appear to be the dominant control on regional stress orientations in the Molasse Basin, the stress field may still be influenced by plate-boundary forces, albeit to a lesser degree.

Implications for hydrocarbon and geothermal production

The numerous wide and highly eccentric breakouts observed in this study suggest that mechanical wellbore instability may be a significant issue for the drilling of hydrocarbon and geothermal wells in the Molasse Basin. The number of breakouts, and thus mechanical instability of the borehole, can be reduced by raising the mud weight and/or altering borehole deviation and azimuth in order to lower the circumferential stress acting on the wellbore (Aadnoy and Chenevery, 1987; Moos and Peska, 1998; Aadnoy, 2003). It is generally considered that vertical boreholes are least stable in strike-slip faulting stress regimes, while wells deviated towards the S_h direction are least stable in thrust faulting stress regimes (Mastin, 1988; Peska and Zoback, 1995). Hence, in the absence of detailed stress magnitudes, we predict that wells deviated towards S_H in the Molasse Basin (i.e. N-S in southeast Germany and NNW-SSE in southwest Germany) are likely to have the lowest absolute stress magnitudes and differential stresses acting upon them and, thus be more mechanically stable.

The present-day state of stress is also a key influence on fluid flow through both natural and hydraulically-induced fractures and is thus of key significance for geothermal and petroleum production in the Molasse Basin. Hydraulically-induced fractures open against the minimum principal stress (typically S_h; Hubbert & Willis, 1957). Hence, hydraulic fractures induced in the Molasse Basin would be expected to strike parallel to S_H (N-S to NNW-SSE) if a strike-slip stress regime is present, or to be sub-horizontal in a thrust faulting stress regime. Natural fractures that are most suitably oriented for tensile or shear failure in the present-day stress tensor, typically those fractures striking parallel to or within 30º of the maximum principal stress respectively, are observed to transmit the greatest volumes of fluids in many fractured rocks (Barton et al., 1995; Sibson, 1996). Hence, any engineered geothermal production planned in fractured reservoirs in the Molasse Basin should target natural fractures that are optimally oriented for failure in the present-day stress tensor, namely sub-vertical fractures that strike between NNW and NNE in a strike-slip stress regime, or fractures that are sub-horizontal or dipping approximately 30 º towards the north or south in a thrust faulting stress regime.

Implications for other foreland basins

The hypothesis that topographic body forces from the Alps may influence the far-field intraplate stress pattern is largely inconsistent with generally accepted theory that large-scale stress patterns are controlled by plate boundary forces (Zoback, 1992; Richardson, 1992; Zoback and Mooney, 2003). However, it is interesting to note that similar stress patterns have been observed from borehole breakout analysis in other foreland basins. Similar regional stress field analysis has also been conducted in the Alberta and Neuquén Basins, foreland basins of the Rockies and Andes respectively, and both reveal S_H orientations that are consistently perpendicular to the strike of the topographic front (Bell, 1996; Guzmán et al., 2007, Guzmán and Cristallini, 2009). The S_H orientations observed in the Alberta and Neuquén Basins, and in the southwest part of the Molasse Basin, are consistent with absolute plate motion and thus have been used to suggest that plate boundary forces, rather than gravitational forces, control the S_H orientation in these foreland areas (Richardson, 1992; Zoback, 1992; Gölke and Coblentz, 1996; Guzmán et al., 2007; Guzmán and Cristallini, 2009). However, the strike of the topographic front is largely perpendicular to the direction of relative plate motion in the Alberta, Neuquén, Cuya and southwest Molasse Basins, and thus both topographic body forces and plate boundary forces may be expected to yield similar S_H orientations. In contrast, the section of the Molasse Basin in southeast Germany provides an opportunity to distinguish between the stress patterns generated by intraplate topographic body forces from that generated by plate boundary forces. Therefore, we suggest that the present-day S_H orientations observed in the Alberta, Cuya and Neuquén Basins may also predominantly reflect intraplate topographic body forces, rather than stresses generated by plate boundary forces. Furthermore, we predict that present-day S_H orientations are likely to be perpendicular to the topographic front in other foreland basins, particularly those that are mechanically detached from the basement.

6. Conclusions

The S_H orientations observed in this study yield the first regional understanding of the stress pattern in the German Molasse Basin. The mean S_H orientation rotates ~30° counterclock-wise from N-S in southeast Germany to NNW-SSW in southwest Germany and the Swiss Molasse Basin and, quite significantly, shows a clear correlation with the strike of the Alpine front (Fig. 2; Fig. 4). We suggest that the gravitational potential energy generated by Alpine topography is the dominant source of stress in the Molasse Basin. Furthermore, N-S S_H orientations are observed over 100 km from the Alps into the Northern Alpine foreland, indicating that the Alpine topography may be a significant source of intraplate stresses in Western Europe.

Acknowledgments

We thank Dr. Thomas Fritzer (LfU, Munich) for his help gathering wellbore data and the Wirtschaftsverband Erdöl- und Erdgasgewinnung for permission to publish the data. Thanks to two anonymous reviewers. Their comments helped clarifying the manuscript. We acknowledge the financial support of the Heidelberg Academy of Sciences and Humanities.

References

Aadnoy, B.S., Chenevery, M.E., 1987. Stability of highly inclined boreholes. SPE Drilling Engineering 2, 364-374.

Aadnoy, B.S., 1990. Inversion technique to determine the in-situ stress field from fracturing data. Journal of Petroleum Science and Engineering 4, 127-141.

Aadnoy, B.S., Bell, J.S., 1998. Classification of drill-induce fractures and their relationship to in-situ stress directions. The Log Analyst 39, 27-42.

Aadnoy, B.S., 2003. Introduction to special issue on borehole stability. J. Pet. Sci. and Eng. 38, 79-82.

Bachmann, G., Dohr, G., Müller, M., 1982. Exploration in a classic thrust and fold belt and its foreland: Bavarian Alps. AAPG Bull. 66, 2529-2542.

Bachmann, G., Müller, M., Weggen, K., 1987. Evolution of the Molasse basin (Germany, Switzerland). Tectonophysics 137, 77-92.

Barton, C.A., Zoback, M.D., Burns, K.L., 1988. In situ stress orientation and magnitude at the Fenton geothermal site, New Mexico, determined from wellbore breakouts. Geophys. Res. Letters 15, 467-470.

Barton, C.A., Zoback, M.D., Moos, D., 1995. Fluid flow along potentially active faults in crystalline rock. Geology 23, 683-686.

Bell, J.S., Gough, D.I., 1979. Northeast-southwest compressive stress in Alberta: Evidence from oil wells. Earth and Planetary Science Letters 45, 475-482.

Bell, J.S., 1990. Investigating stress regimes in sedimentary basins using information from oil industry wireline logs and drilling records. In: Hurst, A., Lovell, M., Morton, A.

(Eds.), Geological applications of wireline logs. Geol. Soc. London Spec. Publ. 48, 305-325.

Bell, J.S., 1996. Petro Geoscience 1. In situ stresses in sedimentary rocks (part 2): applications of stress measurements. Geoscience Canada 23, 135-153.

Betz, D., Wendt, A., 1983. Neuere Ergebnisse der Aufschluß- und Gewinnungstätigkeit auf Erdöl und Erdgas in Süddeutschland. Bull. Ver. schweiz. Petroleum-Geol. u. Ing. 49 (117), 9-36.

Brereton, R., Müller, B., 1991. European stress: contributions from borehole breakouts. Phil. Trans. R. Soc. Lond. A 337, 165-179.

Brink, H.-J., Burri, P., Lunde, A., Winhard, H., 1992. Hydrocarbon habitat and potential of Swiss and German Molasse Basin: A comparison. Eclogae geol. Helv. 85, 715-732.

Cloetingh, S., 1986. Intraplate stresses: a new tectonic mechanism for relative sea-level fluctuations. Geology 14, 617-620.

Engelder, T., 1993. Stress Regimes in the Lithosphere. Princeton, Princeton University Press, 457 p.

Farr, T.G. et al., 2007. The Shuttle Radar Topography Mission. Rev. Geophys., 45 (RG2004), doi:10.1029/2005RG000183.

Gölke, M., Coblentz, D., 1996. Origins of the European regional stress field. Tectonophysics 266, 11-24.

Grünthal, G., Stromeyer, D., 1986. Stress Pattern in Central Europe and Adjacent Areas. Gerlands Beitr. Geophysik, Leipzig, 95, 443-452.

Grünthal, G., Stromeyer, D., 1992. The recent Crustal Stress Field in Central Europe: Trajectories and Finite Element Modeling. J. Geophys. Res., 97 (B8), 11805-11820.

Guzmán, C., Cristallini, E., Bottesi, G., 2007. Contemporary stress orientations in the Andean retroarc between 34ºS and 39ºS from borehole breakout analysis. Tectonics 26, TC3016, doi:10.1029/2006TC001958.

Guzmán, C. G., Cristallini, E.O., 2009. Contemporary stress orientations from borehole breakout analysis in the southernmost flat-slab boundary Andean retroarc (32°44' and 33°40' S), J. Geophys. Res., 114, B02406, doi:10.1029/2007JB005505.

Haimson, B.C., Herrick, C.G., 1989. Borehole breakouts and in situ stress. Proceedings of the 12th Annual Energy Sources Technology Conference, Houston, Texas.

Heidbach, O., Reinecker, J., Tingay, M., Müller, B., Sperner, B., Fuchs, K., Wenzel, F., 2007. Plate boundary forces are not enough: Second- and third-order stress patterns highlighted in the World Stress Map database. Tectonics, 26, TC6014 doi:10.1029/2007TC002133.

Heidbach, O., Tingay, M., Barth, A., Reinecker, J., Kurfeß, D., Müller, B., 2008. The 2008 release of the World Stress Map. (available online at www.world-stress-map.org).

Heidbach, O., Tingay, M., Barth, A., Reinecker, J., Kurfeß, D., Müller, B., this issue. Global spatial wave-length analysis of the tectonic intraplate stress pattern. Tectonophysics.

Heissbauer, H., 1975. Die Gebirgsmechanik beim Abbau in großer Teufe des Kohlebergwerks Peißenberg und ihre Auswirkungen auf die Bergtechnik. Geologica Bavarica 73, 37-53.

Hillis, R.R., Holford, S.P., Green, P.F., Doré, A.G., Gatliff, R.W., Stoker, M.S., Thomson, K., Turner, J.P., Underhill, J.R., Williams, G.A., 2008. Cenozoic exhumation of the southern British Isles. Geology 36(5), 371-374.

Hubbert, M.K., Willis, D.G., 1957. Mechanics of hydraulic fracturing. AIME Petroleum Transactions 210, 153-166.

Huber, K., Schwerd, K., 1995. Das Geologische Profil der Tiefbohrung Hindelang 1 (Allgäuer Alpen). Geologica Bavarica 100, 23-54.

Illies, J.H., Greiner, G., 1978. Rhinegraben and the Alpine system. GSA Bull. 89, 770-782.

Kastrup, U., Zoback, M.L., Deichmann, N., Evans, K.F., Giardini, D., Michael, A.J., 2004. Stress field variations in the Swiss Alps and the northern Alpine foreland derived from inversion of fault plane solutions. J. Geophys. Res. 109, B01402, doi:10.1029/2003JB002550.

Kuhlemann, J., Kempf, O., 2002. Post-Eocene evolution of the North Alpine Foreland Basin and its response to Alpine tectonics. Sedimentary Geology 152, 45-78.

Mardia, K.V., 1972. Statistics of directional data: probability and mathematical statistics. Academic Press, London, 357 pp.

Mastin, L., 1988. Effect of borehole deviation on breakout orientations. J. Geophys. Res. 93, 9187-9195.

Moos, D., Peska, P., 1998. Predicting the stability of horizontal wells and multilaterals - the role of in situ stress and rock properties. SPE International conference on horizontal well technology.

Müller, B., Zoback, M.L., Fuchs, K., Mastin, L., Gregersen, S., Pavoni, N., Stephansson, O., Ljunggren, Ch., 1992. Regional pattern of tectonic stress in Europe. J. Geophys. Res. 97, 11783-11803.

Müller, B., Wehrle, V., Zeyen, H., Fuchs, K., 1997. Short-scale variations of tectonic regimes in the western European stress province north of the Alps and Pyrenees. Tectonophysics 275, 199-219.

Müller, B., Wehrle, V., Hettel, S., Sperner, B., Fuchs, F., 2003. A new method for smoothing oriented data and its application to stress data. In: M. Ameen (Editor), Fracture and In-situ Stress Characterization of Hydrocarbon Reservoirs. Special Publication. Geological Society, London, pp. 107-126.

Müller, M., Nieberding, F., 1995. Die überhydrostatischen Porendrücke in der Bohrung Hindelang 1 (Allgäuer Alpen) und ihre Beziehung zur Umgebung. Geologica Bavarica 100, 167-174.

Müller, M., Nieberding, F., 1995. Principles of abnormal pressure related to tectonic developments and their implication for drilling activities (Bavarian Alps, Germany). In: G. Wessley and W. Liebl (eds), Oil and gas in Alpidic thrustbelts and basins of Central and Eastern Europe. EAGE special publication, 5, 119-126.

Peska, P., Zoback, M.D., 1995. Compressive and tensile failure of inclined wellbores and determination of in situ stress and rock strength. J. of Geophys. Res. 100, 12791-12811.

Plumb, R.A., Hickman, S.H., 1985. Stress-induced borehole elongation: a comparison between the four-arm dipmeter and the borehole televiewer in the Auburn geothermal well. J. Geophys. Res. 90, 5513-5521.

Reinecker, J., Lenhardt, W.A., 1999. Present-day stress field and deformation in Eastern Austria. Int. Journ. Earth Sciences, 88, 532-550.

Reinecker, J., Tingay, M., Müller, B., 2003. Borehole breakout analysis from four-arm caliper logs. World Stress Map Project Stress Analysis Guidelines (available online at www.world-stress-map.org).

Reinecker, J., Heidbach, O., Tingay, M., Sperner, B., Müller, B., 2005. The 2005 release of the World Stress Map.

Richardson, R.M., 1992. .Ridge forces, absolute plate motions, and the intraplate stress field. Journal of Geophysical Research, 97, 11739-11748.

Schrader, F., 1988. Das regionale Gefüge der Drucklösungsdeformation an Geröllen im westlichen Molassebecken. Geol. Rdsch. 77, 347-369.

Sibson, R.H., 1996. Structural permeability of fluid-driven fault-fracture meshes. J. of Struct.l Geo. 18, 1031-1042.

Sonder, L.J., 1990. Effects of density contrasts on the orientation of stresses in the lithosphere: relation to principal stress direction in the Transverse Ranges, California. Tectonics 9(4), 761-771.

Tingay, M., Müller, B., Reinecker, J., Heidbach, O., 2006. State and origin of the present-day stress field in sedimentary basins: New results from the World Stress Map project. 41st U.S. Rock Mech. Symp., Golden Rocks 2006, Golden/Colorado, 17.-21.6.2006, published plenary paper ARMA/USRMS 06-1049.

Tingay, M., Reinecker, J., Müller, B., 2008. Borehole breakout and drilling-induced fracture analysis from image logs. World Stress Map Project Stress Analysis Guidelines (available online at www.world-stress-map.org).

Trümpy, R., 1980. Geology of Switzerland, Part A: An Outline of the Geology of Switzerland. 104 p., Wepf & Co. Publishers (Basel).

Zajak, B.J., Stock, J.M., 1997. Using borehole breakouts to constrain the complete stress tensor: Results from the Siljan Deep Drilling Project and offshore Santa Maria Basin, California. J. Geophys. Res. 102, 10083-10100.

Ziegler, P.A., 1987. Late Cretaceous and Cenozoic intra-plate compressional deformations in the Alpine foreland – a geodynamic model. Tectonophysics 137, 389-420.

Ziegler, P.A., 1990. Geological Atlas of Western and Central Europe 1990. Shell Internationale Petroleum Maatschappij, Den Haag, The Netherlands, 239 p.

Zoback, M.D., Moos, D., Mastin, L.G., Anderson, R.N., 1985. wellbore breakouts and in situ stress. J. of Geophys. Res. 90, 5523-5530.

Zoback, M.L., 1992. First- and second-order patterns of stress in the lithosphere: The world stress map project. J. of Geophys. Res. 97, 11703-11728.

Zoback, M.L., Mooney, W.D., 2003. Lithospheric buoyancy and continental intraplate stresses. Int. Geology Rev. 45, 95-118.

Figure captions

Figure 1. (A) Overview of the Swiss-German Molasse Basin with contour lines of the base of Tertiary sediments (i.e. the Molasse sediments) and major structures **(B)** N-S profile through the German Molasse Basin.

Figure 2. Present-day orientation of maximum horizontal stress (S_H) determined in this study from borehole breakouts and drilling-induced fractures. Symbol size is proportional to quality of the data. Names identify the wellbore locations according to Table 1. **(A)** A-D quality stress orientations (long axes of symbols) in 96 wells across the German Molasse Basin demonstrate that the present-day S_H in the German Molasse Basin is predominantly oriented N-S. However, localized stress perturbations are observed in Hindelang, Illmensee, Mönchsrot, Tacherting and Vorderiss. **(B)** Detailed view of stress orientations in southeast Germany (same legend as in A). Topography data are from the SRTM project (Farr et al., 2007). **(C)** Rose diagram of the S_H orientations from Fig. 2a. Petal length represents the relative number of wells clustered in 10° azimuthal bins. The overall mean of the maximum horizontal stress orientation ($\overline{S}_H$) and standard deviation (s.d.) for each dataset was calculated using the Mardia statistics for bi-polar data (Mardia, 1972). Note that the standard deviation significantly decreases when D-quality data are omitted.

Figure 3. Occurrence of stress induced borehole failure in the German Molasse Basin with depth, S_H orientation, and level of differential stress depending on **(A and B)** latitude and **(C and D)** longitude. Occurrence with depth is indicated by the vertical bars. The quality of S_H orientation is color coded (see inset). Ratio of BO length to log length as a proxy for differential stress is generally high. There is no significant stress rotation with depth within the entire Molasse Basin. Also there is no significant change in stress down into the pre-

Tertiary basement. The labeled wells are further discussed in the text. Note that the thick grey dashed lines give only a rough orientation for the base of Tertiary and the front of Alpine nappes. Both vary along strike of the Alpine front. The base of Tertiary is up to 3 km higher in the western German Molasse basin than indicated in (A). Here a representative depth is given for the eastern part (comparable to the profile given in Figure 1), where most well bores are located.

Figure 4. Present-day S_H orientations in the Molasse Basin from the analysis herein and from the 2005 World Stress Map database (Reinecker et al., 2005). S_H rotates from N-S in the Eastern Alps (000ºN ± 23º) to NNW-SSE in the Western Alps (150ºN ± 24º). Legends for rose diagrams are the same as in Fig.2. The S_H orientation is roughly perpendicular to the topographic front throughout the basin, indicating that forces originating from the gravitational potential energy of the Alps (rather than plate boundary forces) are controlling the Molasse Basin stress field. See inset legend for details on data types, stress regime (NF = normal faulting, SS = strike-slip, TF = thrust faulting, U = undefined), and quality ranking. Thin black lines are the trajectories of maximum horizontal stress calculated using a quality and distance weighted approach with a smoothing radius of 100 km (as described in Müller et al., 2003).

Table Captions

Table 1. Summary of breakout and drilling-induced fracture analysis results from 132 wells in the German Molasse Basin sorted by longitude. S_H = average maximum horizontal stress orientation (ºN). # = number of breakouts (BO) or drilling-induced fractures (DIF), s.d. = standard deviation, total = total length of BO/DIF, top and bottom =

shallowest/deepest BO/DIF observed in well. Data are included in World Stress Map 2008 database release (Heidbach et al, 2008).

Figure_01
Click here to download high resolution image

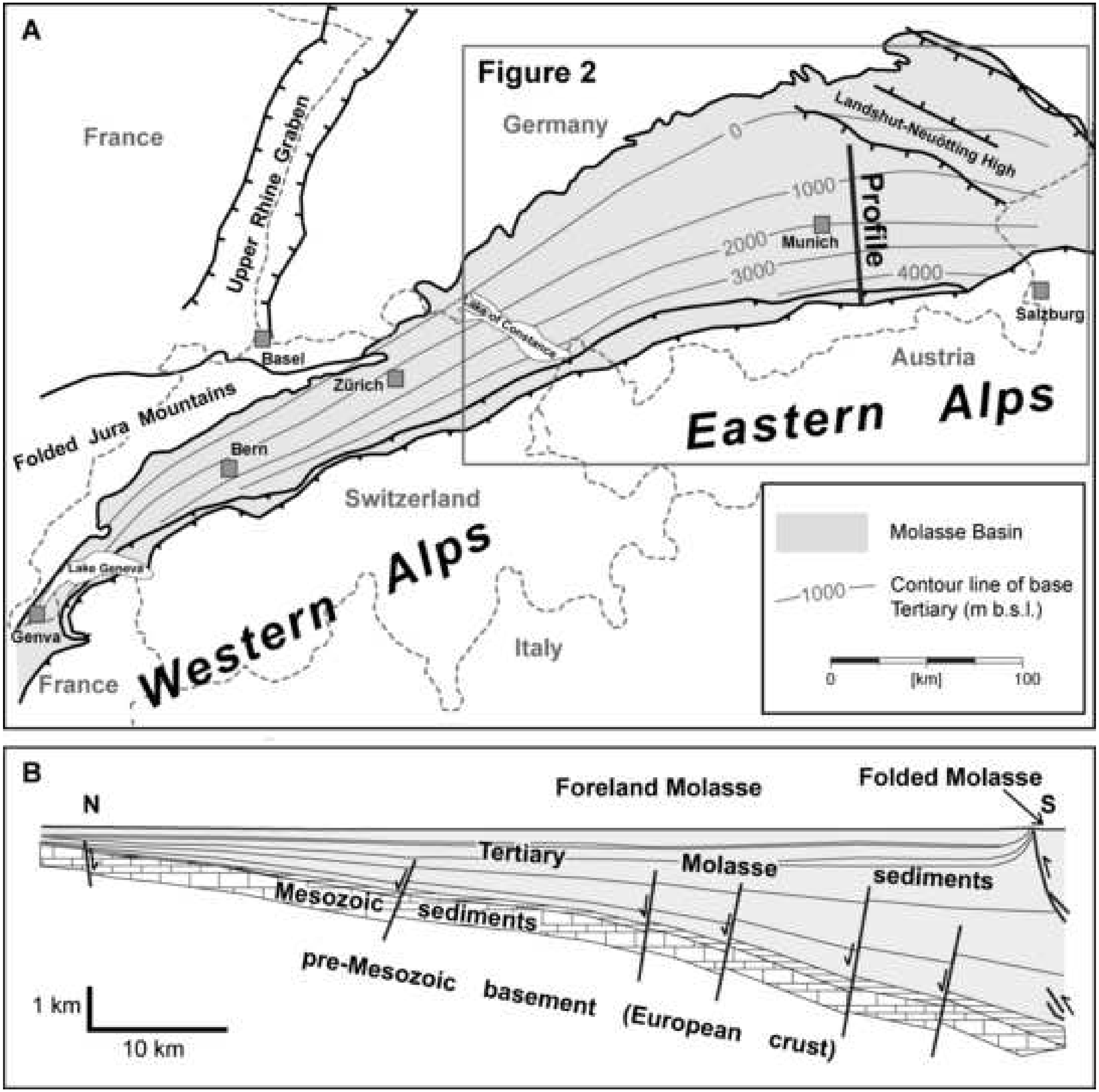

Figure_02

Click here to download high resolution image

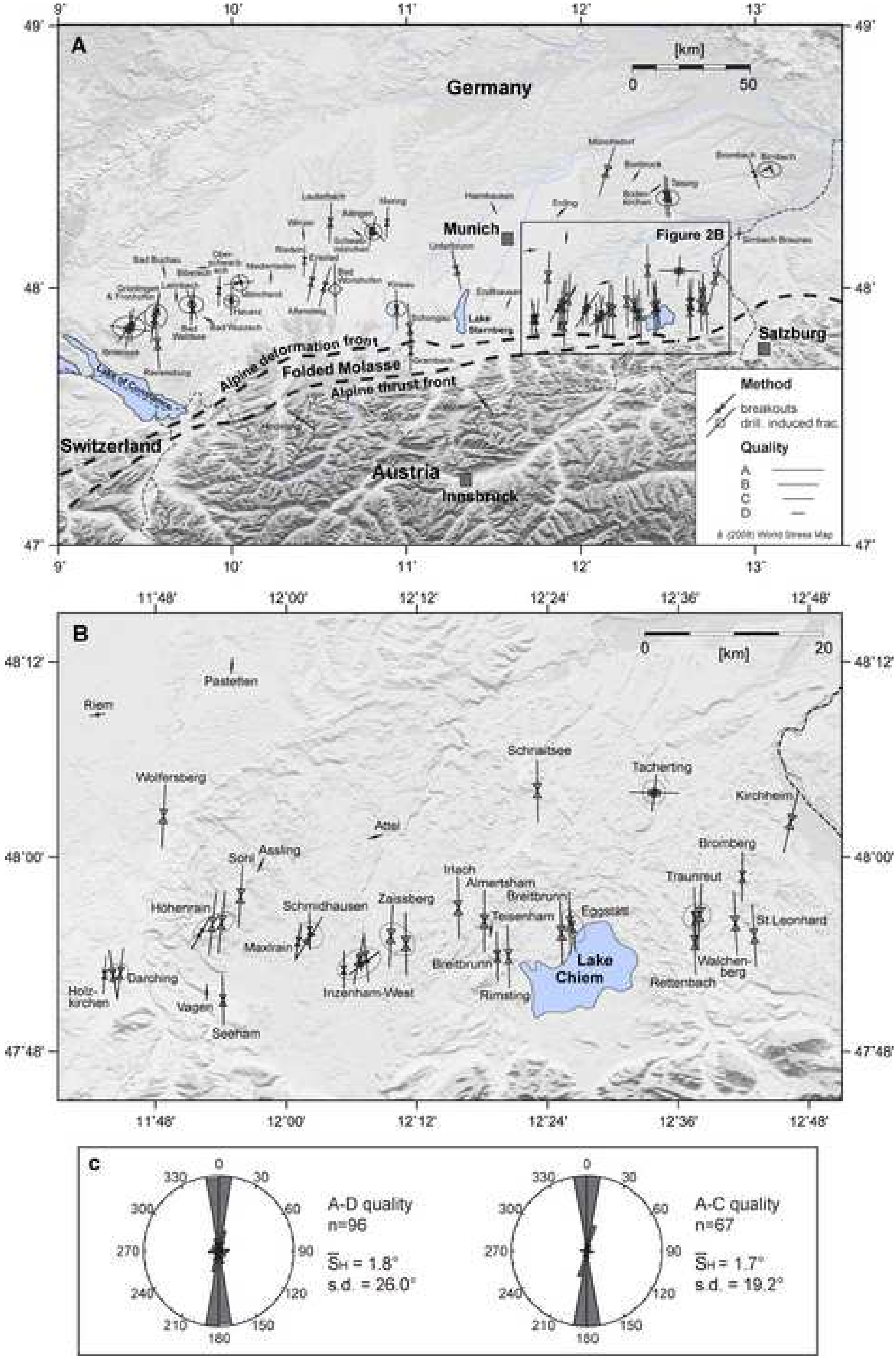

Figure_03

Click here to download high resolution image

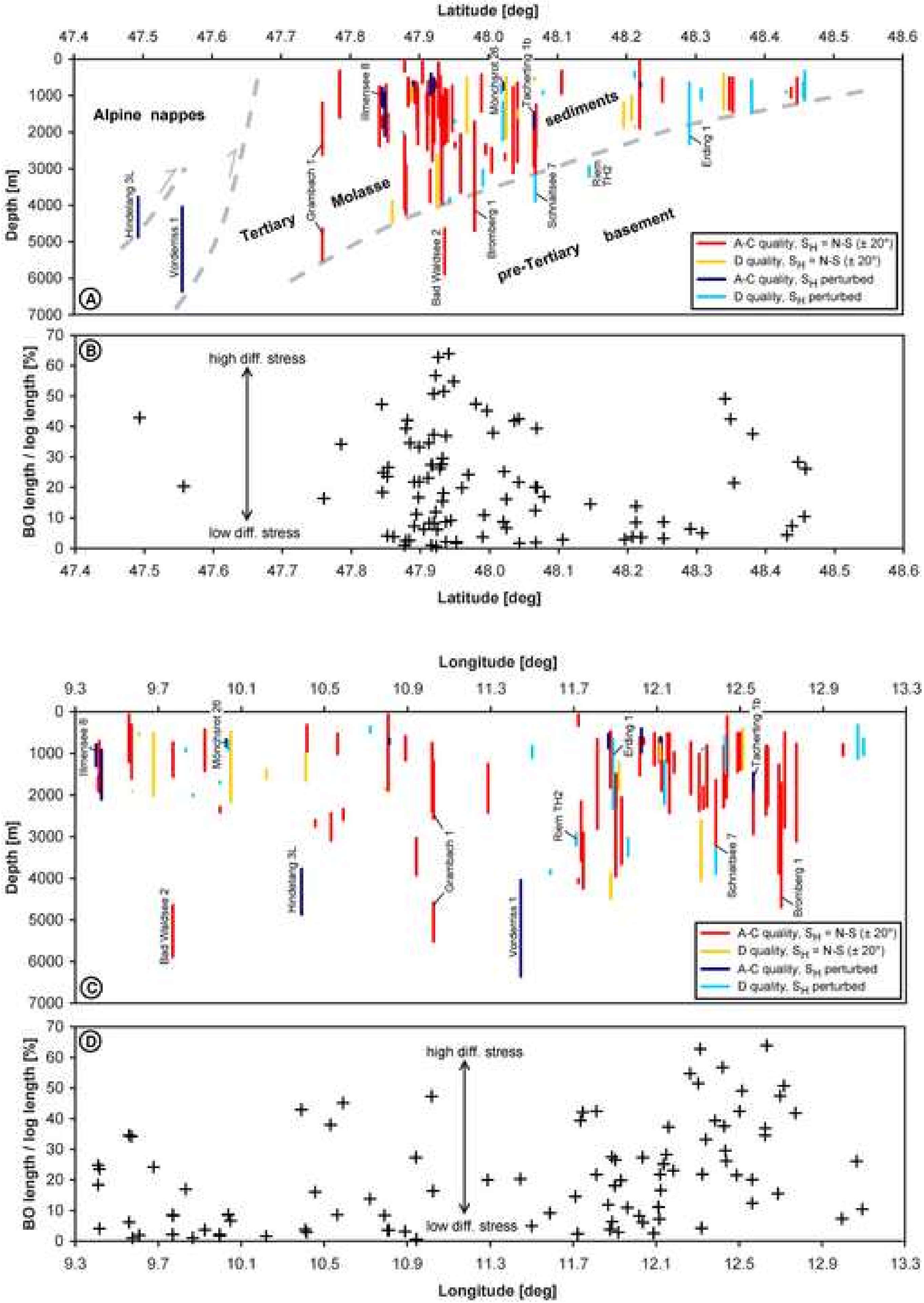

Figure_04

Click here to download high resolution image

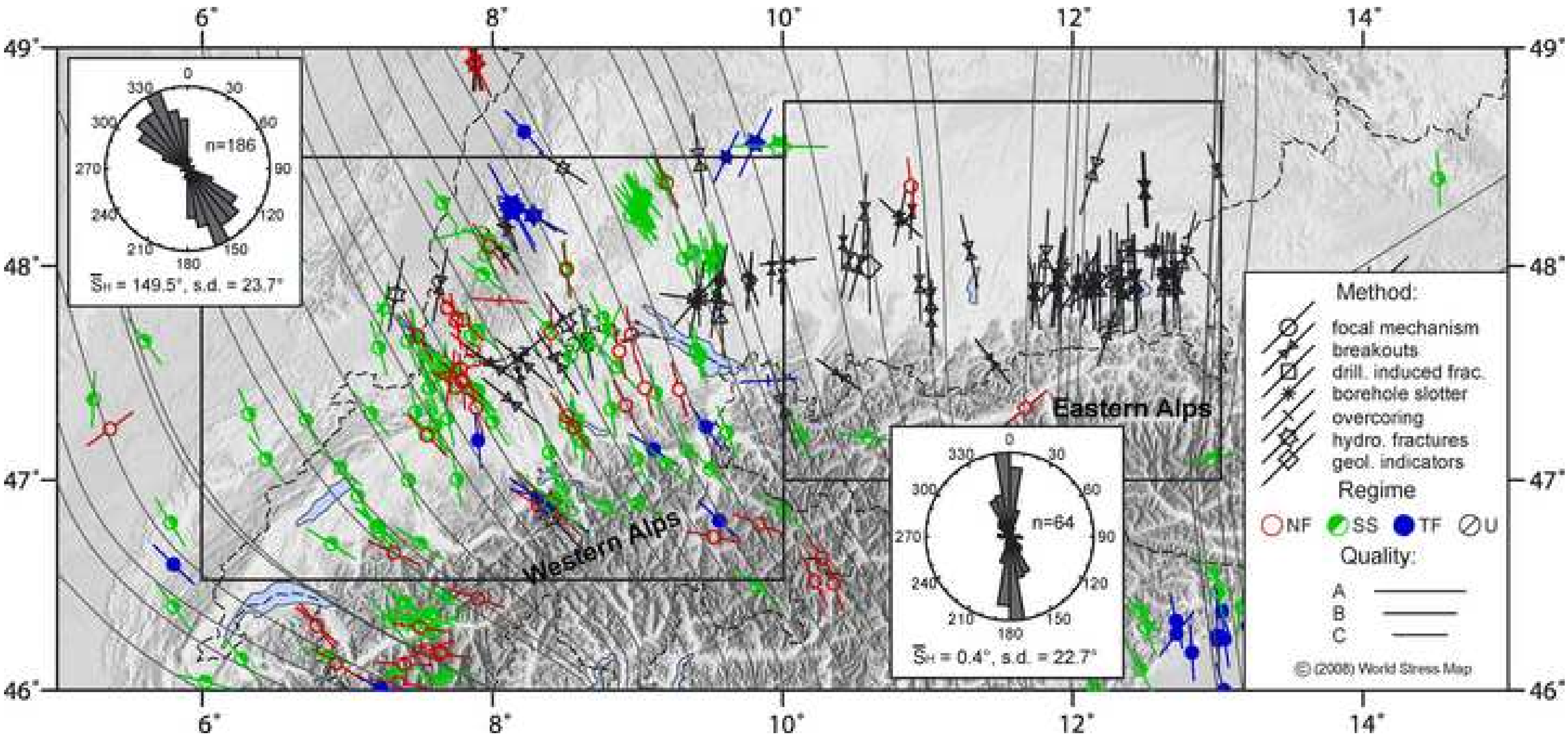

Table_01
Click here to download Table: Table_1_final.doc

Table 1.

lat	long	S_H	Type	Depth [km]	Quality	Locality	#	s.d.	Total [m]	Top [m]	Bottom [m]
47.846	9.41	11	BO	1.7	B	Illmensee 7	4	9	169	1558	1878
47.845	9.41	98	BO	1.0	B	Illmensee 8	9	7	170	785	1304
47.852	9.416	40	BO	1.5	B	Illmensee 5	8	20	364	916	2099
47.852	9.416	177	BO	1.3	C	Illmensee 6	12	16	66	703	1930
47.885	9.559	10	BO	0.9	A	Grünlingen 1	38	11	344	518	1200
47.905	9.559	11	BO	0.4	B	Fronhofen 16	9	10	111	74	645
47.785	9.571	176	BO	1.0	A	Ravensburg 1	19	7	490	319	1598
47.916	9.575	165	BO	1.9	D	Fronhofen 23	1	-	5	1904	1908
48.067	9.607	172	BO	0.5	D	Bad Buchau	2	10	10	508	554
47.969	9.677	177	BO	1.3	D	Laimbach 1	30	27	296	510	2021
47.937	9.769	5	DIF	5.1	C	Bad Waldsee 2	7	16	31	4641	5563
47.937	9.769	161	BO	5.3	C	Bad Waldsee 2	25	20	123	4674	5879
47.919	9.771	5	BO	1.1	C	Bad Waldsee 1	6	5	79	737	1556
48.079	9.832	87	BO	0.9	D	Jordanbad Biberach 1	2	10	30	887	945
47.877	9.866	121	BO	2.0	D	Bad Wurzach 3	3	7	15	1993	2018
47.99	9.924	2	BO	0.9	C	Oberschwarzach 4	4	7	45	426	1420
47.99	9.932	-	BO	-	E	Oberschwarzach 3	-	-	-	-	-
47.952	9.996	100	BO	1.7	D	Hauerz 3	1	-	32	1680	1712
47.952	9.997	2	BO	2.3	C	Hauerz 1	5	2	33	2288	2411
47.953	10.011	-	BO	-	E	Hauerz 2	-	-	-	-	-
48.02	10.036	83	BO	0.7	C	Mönchsrot 26	12	15	97	664	829
48.02	10.036	81	BO	0.8	D	Mönchsrot 26A	8	32	76	690	916
48.024	10.048	161	BO	1.3	D	Mönchsrot 27	13	37	126	485	2171
48.224	10.172	-	BO	-	E	Buch 1	-	-	-	-	-
48.043	10.22	0	BO	1.5	D	Niederrieden 1	2	0	5	1383	1599
48.061	10.246	-	BO	-	E	Lauberhart 3	-	-	-	-	-
48.061	10.246	-	BO	-	E	Lauberhart 1	-	-	-	-	-
48.071	10.248	-	BO	-	E	Lauberhart 2	-	-	-	-	-
48.112	10.365	-	BO	-	E	Arlesried 11	-	-	-	-	-
48.113	10.38	-	BO	-	E	Arlesried 29	14	46	405	423	1337
47.493	10.389	125	BO	4.3	C	Hindelang 3L	15	22	505	3778	4866
48.207	10.409	175	BO	1.3	D	Winzer 1	2	0	56	1012	1653
48.106	10.415	2	BO	0.6	C	Rieden 3	8	3	33	323	947
48.024	10.456	11	BO	2.7	B	Erisried 1	4	2	121	2597	2748
48.005	10.531	16	BO	2.7	B	Altensteig 1	10	17	288	2435	3090
48.252	10.563	3	BO	0.7	B	Lauterbach 1	14	7	102	526	1010
47.996	10.591	178	DIF	2.4	A	GT2 Bad Worishofen	22	6	122	2337	2596
48.152	10.602	-	BO	-	E	Zaisertshofen 5	-	-	-		
48.212	10.721	130	BO	0.4	D	Schwabmünchen 4	2	26	135	355	497
48.212	10.791	174	BO	1.85	D	Aitingen 1	2	2	6	1843	1859
48.218	10.795	-	BO	-	E	Aitingen 5	-	-	-	-	-
48.221	10.8	-	BO	-	E	Aitingen 6	-	-	-	-	-
48.219	10.806	12	BO	1.0	C	Aitingen 2	18	10	70	67	1890
48.22	10.812	132	BO	0.7	C	Aitingen 4a	4	15	26	647	760
48.22	10.812	-	BO	-	E	Aitingen 4	-	-	-	-	-
48.252	10.89	3	BO	0.9	C	Mering 1	8	8	40	591	1157
47.91	10.923	-	BO	-	E	Kinsau 2	-	-	-	-	-
47.916	10.942	178	BO	3.4	B	Kinsau 1	8	7	250	3035	3916
47.923	10.945	165	BO	3.2	D	Kinsau 3	1	-	2	3224	3226
47.844	11.018	176	BO	1.5	A	Schongau 1	39	8	828	752	2382
47.76	11.025	1	BO	3.3	B	Grambach 1	52	17	711	1192	5509
48.069	11.287	167	BO	1.8	B	Unterbrunn 3	9	4	354	1248	2418
48.286	11.442	-	DIF	-	E	Hebertshausen 4a	2	0	1	1555	1565
48.286	11.442	-	BO	-	E	Hebertshausen 1	-	-	-	-	-
47.557	11.445	142	BO	5.1	C	Vorderriss 1	60	27	490	4043	6353
48.308	11.5	155	BO	0.9	D	Haimhausen 1 and 1a	2	0	52	822	1097
48.312	11.531	-	BO	-	E	Haimhausen 2	-	-	-	-	-
47.944	11.587	24	BO	3.8	D	Endlhausen 1	5	11	23	3808	3887
48.146	11.711	81	DIF	3.1	D	Riem TH2	18	40	44	2935	3206
47.879	11.722	4	BO	2.0	C	Holzkirchen 3	6	11	66	71	4107
47.879	11.735	171	BO	3.1	B	Darching 5	16	14	970	2155	3575
47.881	11.746	7	BO	3.6	B	Darching 3	31	21	1017	2910	4240
48.042	11.812	3	BO	1.7	A	Wolfersberg 11	42	7	1002	653	2812
48.042	11.812	3	BO	1.3	A	Wolfersberg 10a	18	3	517	695	1927
48.042	11.812	35	BO	1.2	E	Wolfersberg 9	37	48	321	700	1802
48.105	11.813	-	BO	-	E	Poering 1	-	-	-	-	-
47.796	11.839	-	BO	-	E	Miesbach 1	-	-	-	-	-
47.922	11.869	30	BO	0.7	C	Höhenrain A5	4	17	166	535	868
47.922	11.869	-	BO	-	E	Höhenrain H1	-	-	-	-	-
47.861	11.878	0	BO	4.2	D	Vagen 1	2	0	40	3890	4478
47.931	11.887	7	BO	1.2	A	Höhenrain 4	20	4	541	470	1822
48.291	11.888	43	BO	1.5	D	Erding 1	22	40	114	644	2323
47.933	11.901	6	BO	2.8	A	Höhenrain 6	27	8	366	1962	3950
47.853	11.903	179	BO	1.8	B	Seeham C1	9	3	432	1491	2260

48.196	11.917	4	BO	1.5	D	Pastetten 1	3	4	31	1201	1864
47.96	11.93	4	BO	2.8	A	Söhl 1	13	4	413	2057	3648
47.992	11.961	25	BO	3.2	D	Assling 5	7	27	199	3037	3460
47.992	11.961	-	BO	-	E	Assling 5a	-	-	-	-	-
47.913	12.018	8	BO	1.0	C	Maxlrain A1	6	4	94	606	1518
47.917	12.035	32	BO	0.7	B	Schmidhausen A3	7	5	166	403	970
47.924	12.036	179	BO	0.7	C	Schmidhausen A2	8	3	40	629	768
47.919	12.068	-	BO	-	E	Schmidhausen-Ost C1	-	-	-	-	-
47.884	12.088	0	BO	0.8	C	Inzenham-West 3	13	7	27	518	1280
48.33	12.089	-	BO	-	E	Hofkirchen 2	-	-	-	-	-
47.893	12.092	-	BO	-	E	Inzenham-West 2	-	-	-	-	-
47.892	12.105	108	BO	0.8	E	Inzenham-West 11	2	3	68	645	923
47.894	12.111	11	BO	1.0	B	Inzenham-West 4	12	3	94	620	1198
47.886	12.112	-	BO	-	E	Inzenham-West 42	-	-	-	-	-
47.891	12.115	4	BO	1.0	D	Inzenham-West 23	3	7	58	775	1145
47.891	12.119	52	BO	0.7	C	Inzenham-West 14	12	11	73	608	866
47.897	12.122	174	BO	1.2	B	Inzenham-West C5	11	6	223	656	1892
48.021	12.136	73	BO	1.7	D	Attel 3	13	43	303	1180	2213
48.447	12.149	17	BO	0.8	A	Münchsdorf 1	18	8	314	519	1191
47.919	12.16	3	BO	1.5	A	Zaissberg C4	14	5	926	525	2420
47.911	12.183	179	BO	1.2	A	Zaissberg C3	18	4	231	970	1450
47.948	12.263	179	BO	1.3	A	Irlach C1	11	2	704	731	1966
47.929	12.298	-	BO	-	E	Almertsham C2	-	-	-	-	-
47.934	12.303	0	BO	1.7	A	Almertsham C1	32	4	755	1010	2375
47.926	12.313	7	BO	3.3	D	Teisenham 1	16	32	925	2602	4044
48.431	12.319	30	BO	0.9	D	Bonbruck 2	1	-	23	887	910
47.898	12.323	179	BO	2.1	B	Breitbrunn C4	16	3	151	1800	2328
47.898	12.34	178	BO	1.5	A	Rimsting C1	15	12	494	814	2273
47.91	12.358	-	BO	-	E	Breitbrunn C5	-	-	-	-	-
48.068	12.384	1	BO	2.2	A	Schnaitsee 7	14	8	926	1640	2793
48.068	12.384	147	BO	3.8	D	Schnaitsee 7	2	3	58	3733	3869
47.912	12.407	-	BO	-	E	Breitbrunn C1	-	-	-	-	-
47.922	12.421	178	BO	1.5	A	Breitbrunn C10	24	5	1020	834	2286
47.928	12.426	-	BO	-	E	Eggstätt C1	-	-	-	-	-
48.381	12.428	48	BO	1	D	Bodenkirchen 1 - 1a	15	46	454	575	1463
47.932	12.434	178	BO	1.5	A	Eggstätt C2	19	10	341	1325	2066
47.923	12.435	-	BO	-	E	Breitbrunn 22	-	-	-	-	-
47.923	12.435	-	BO	-	E	Breitbrunn 21	-	-	-	-	-
47.923	12.435	-	BO	-	E	Breitbrunn 26	-	-	-	-	-
47.923	12.435	-	BO	-	E	Breitbrunn C6	-	-	-	-	-
47.928	12.438	172	BO	1.0	B	Eggstätt C4	17	13	249	105	1583
48.354	12.488	177	BO	0.9	B	Teising 1	10	4	167	507	1442
48.349	12.502	177	BO	0.9	B	Teising 2	12	19	456	506	1381
48.341	12.514	172	BO	0.9	D	Teising 3	19	35	512	412	1376
47.9	12.544	-	BO	-	E	Chieming C1	-	-	-	-	-
48.066	12.563	91	BO	1.6	B	Tacherting 1-b	5	2	259	1465	1890
48.066	12.563	6	BO	2.4	C	Tacherting 1-a	2	6	419	1900	2936
48.141	12.585	-	BO	-	E	Garching 1	-	-	-	-	-
47.912	12.625	178	BO	1.7	A	Rettenbach C2	27	6	635	887	2478
47.937	12.626	178	BO	1.6	A	Traunreut A3	25	4	591	814	2321
47.941	12.633	3	BO	1.5	A	Traunreut A2	21	4	1185	852	2258
48.158	12.641	-	BO	-	E	Hinterberg 2	-	-	-	-	-
47.985	12.649	-	BO	-	E	Traunreut C1	-	-	-	-	-
47.932	12.687	177	BO	2.5	A	Walchenberg 1	11	8	397	1269	3878
47.98	12.698	1	BO	3.2	B	Bromberg 1	54	20	1716	1713	4690
48.177	12.704	-	BO	-	E	Pirach 1	-	-	-	-	-
47.919	12.716	176	BO	1.6	A	St.Leonhard C1	31	4	1435	492	2778
48.036	12.772	13	BO	2.4	A	Kirchheim C1	27	6	1017	768	3112
48.338	12.777	-	BO	-	E	Wurmannsquick 1	-	-	-	-	-
48.299	12.965	-	BO	-	E	Taubenbach 1	-	-	-	-	-
48.438	12.996	160	BO	0.9	C	Brombach 1	15	11	69	783	1044
48.258	13.01	5	DIF	1.8	D	Simbach-Braunau TH1	10	8	11	1770	1839
48.458	13.067	60	BO	0.7	D	Birnbach 5	16	41	265	328	1127
48.456	13.094	152	BO	0.8	D	Birnbach T 4	7	32	71	648	1042